ANL/CHM/CP-99495 Invited Talk, SPIE, Liquid Crystals III
Denver, Colorado July 21-22, 1999

Photorefractivity in liquid crystals doped with a soluble conjugated polymer

Gary P. Wiederrecht[a], Walter A. Svec[a], Mark P. Niemczyk[a], and Michael R. Wasielewski[b]

[a]Chemistry Division, Argonne National Laboratory, Argonne, IL 60439-4831

[b]Department of Chemistry, Northwestern University, Evanston, IL 60208-3113

ABSTRACT

Photoconductive polymers are doped into liquid crystals to create a new mechanism for space-charge field formation in photorefractive liquid crystal composites. The composites contain poly(2,5-bis(2'-ethylhexyloxy)-1,4-phenylenevinylene) (BEH-PPV) and the electron acceptor N,N'-dioctyl-1,4:5,8-naphthalenediimide, NI. Using asymmetric energy transfer (beam coupling) measurements that are diagnostic for the photorefractive effect, the direction of beam coupling as a function of grating fringe spacing inverts at a spacing of 5.5 μm. We show that the inversion is due to a change in the dominant mechanism for space-charge field formation. At small fringe spacings, the space-charge field is formed by ion diffusion in which the photogenerated anion is the more mobile species. At larger fringe spacings, the polarity of the space charge field inverts due to dominance of a charge transport mechanism in which photogenerated holes are the most mobile species due to hole migration along the BEH-PPV chains coupled with interchain hole hopping. Control experiments are presented, which use composites that can access only one of the two charge transport mechanisms. The results show that charge migration over long distances leading to enhanced photorefractive effects can be obtained using conjugated polymers dissolved in liquid crystals.

Keywords: Liquid Crystals, Photorefractive Materials, Photoconductive Polymers

1. INTRODUCTION

The photorefractive effect is a light-induced change in the refractive index of a nonlinear optical material that results from the creation of a spatially periodic electric field (space-charge field). This space-charge field is produced by photoinduced charge separation within the illuminated regions of an optical interference pattern of fringe spacing Λ created in the material by two coherent, crossed laser beams as illustrated in Figure 1. This is followed by charge migration of the most mobile charge carrier over micron distances into the dark regions of the interference pattern to produce a refractive index grating. Thus, observation of photorefractive effects in a material depend on high optical nonlinearity coupled with efficient charge transport characteristics.

As a consequence of the outstanding optical quality and commercial availability of inorganic ferroelectric materials such as barium titanate and lithium niobate, photorefractive holographic data storage systems have been designed and developed to the point that commercialization of these systems is now being attempted [1]. Although these materials perform well, the availability of materials that are useful over a wide range of wavelengths and have significantly lower cost would dramatically enhance the versatility of the photorefractive effect. In this pursuit, the 1990's have seen the advent of photorefractive polymers and liquid crystals.[2-23] These materials have many attractive properties, such as low dielectric constants, which minimize dielectric shielding of the space charge field, low cost, and relatively simple syntheses. However, the development of useful organic materials is challenging because photorefractivity requires the simultaneous optimization of electro-optic properties, charge generation efficiency, charge transport over macroscopic distances, and charge trapping. Nonetheless, organic materials have been developed to the point that their photorefractive effects by some measures are now larger than those exhibited by their inorganic counterparts.

One of the reasons for large photorefrative effects in organic materials is the molecular orientational capabilities of low glass transition polymers and liquid crystals.[13] For example, nematic liquid crystals reorient easily in weak electric fields and their high birefringence provides an efficient electro-optic mechanism that makes them excellent candidates for photorefractive materials.[7-9, 16-18] The liquid crystal molecules modulate the index of refraction by reorienting to a larger or smaller degree as the modulated space charge field increases or decreases. However, inducing efficient charge transport in

DISCLAIMER

DISCLAIMER

Portions of this document may be illegible in electronic image products. Images are produced from the best available original document.

these materials is not as straightforward, and previous studies rely on photoinduced heterolytic cleavage of dye molecules or intermolecular electron transfer to create mobile anions and cations. This is followed by ion diffusion to create a space-charge field with the magnitude:[8, 24]

$$E_{sc} = \frac{-k_B TK}{2e_o} \frac{D^+ - D^-}{D^+ + D^-} \frac{\sigma_{ph}}{\sigma_{ph} + \sigma_d} \sin Kx \qquad (1)$$

Here, σ_{ph} is the photoconductivity, σ_d is the dark conductivity, k_B is the Boltzmann constant, K is the grating wavevector, x is the direction along the wavevector, ε_o is the charge of the electron, and D^+ and D^- are the diffusion constants for the cations and anions, respectively. This equation assumes that the intensities of the two incident beams are equal (I_1=I_2). It is clear that the two factors which determine the magnitude of the space charge field are the difference in the photoconductivity versus dark conductivity and the difference in the diffusion coefficients of the cations and anions. These factors permit one set of charges to preferentially remain in the illuminated regions of the interference pattern and for the opposing charges to migrate into the nulls of the interference pattern. It should be noted that the photorefractive gain can actually increase at larger fringe spacings, even though the value of E_{SC} decreases with increasing fringe spacing as indicated in Equation 1. This is due to the fact that the orientational response in pure nematic liquid crystals increases as the fringe spacing increases, and the effective electro-optic response also increases.[24]

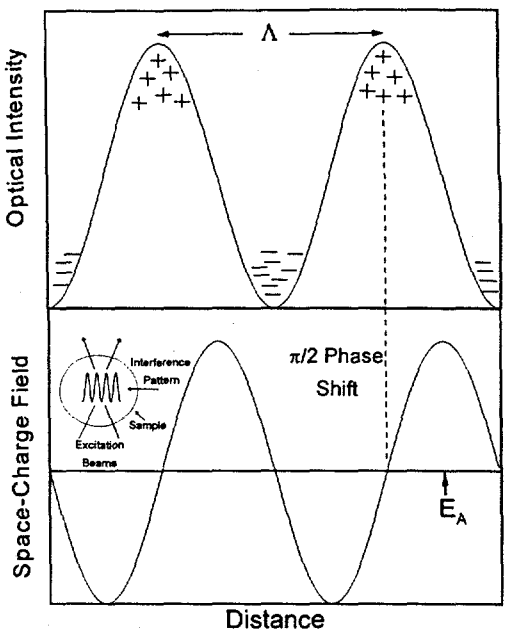

Figure 1 - An illustration of the photorefractive effect. Two laser beams are spatially overlapped in the sample producing an interference pattern (inset). A spatial modulation of charge density is created that produces a space charge field phase shifted by π/2. In an electro-optic material, a refractive index grating results.

In principal, other charge conduction mechanisms are available that can contribute to the creation of a space charge field. Mobile charges obey the current density (J) equations given by: [25, 26]

$$J = J^+ + J^- \qquad (2)$$

$$J^{\pm} = q\mu^{\pm} n^{\pm}(x,t)\left(E_{SC}(x,t) - E_A\right) \mp qD^{\pm} \frac{\partial n^{\pm}[x,t]}{\partial x} \qquad (3)$$

where $\mu^{\pm}$ is the mobility of the cations and anions, x is the grating wavevector axis, $n^{\pm}(x,t)$ is the ion density, $E_{SC}(x,t)$ is the magnitude of the space-charge field, E_A is the magnitude of the applied field, q is the unit charge, and $D^{\pm}$ is the diffusion constant of the cations and anions, respectively. The first term on the right hand side of equation 3 describes charge drift, and the second term describes ion diffusion. As indicated above, previous studies of photorefractivity in liquid crystals indicate rely on ion diffusion is the charge transport mechanism that creates the space-charge field, a process that limits the efficiency and speed of the effect. The charge drift mechanism has not been a factor because of the generally short ionic drift length, L_E, given by:

$$L_E = \frac{\mu^{\pm} \tau^{\pm} V}{d} \qquad (4)$$

where $\tau^{\pm}$ is the carrier lifetime, V is applied potential, and d is the cell thickness.[25] Typically, $2\pi L_E << \Lambda$ in liquid crystals, while the drift mechanism can only contribute to a photorefractive grating if $2\pi L_E \geq \Lambda$.[25]

We now report experimental results for a photorefractive nematic liquid crystal composite containing the conjugated polymer poly(2,5-bis(2'-ethylhexyloxy)-1,4-phenylenevinylene), BEH-PPV, Figure 2. BEH-PPV is well known for its fast, through bond charge transport capabilities.[27] We observe a novel fringe spacing dependent inversion of the polarity of the space-charge field that we interpret as a competition between conventional ionic diffusion and through bond charge transport mechanisms.

2. EXPERIMENTAL METHODS

The molecules used for this study are illustrated in Figures 2 and 3. A eutectic mixture of 35% (weight %) 4'-(*n*-octyloxy)-4-cyanobiphenyl, 8OCB and 65% 4'-(n-pentyl)-4-cyanobiphenyl, 5CB was doped with 10^{-5} M BEH-PPV (200 kD by GPC), as the electron donor.[28] The molecular weight of the BEH-PPV polymer implies that 500 repeat units of the monomer are present with an extended chain length of 0.35 μm. N,N'-dioctyl-1,4:5,8-naphthalenediimide, NI, $8x10^{-3}$ M, was added as the electron acceptor.[29] Two other liquid crystal composites were also studied as controls. The first control composite contains the 5 unit phenylenevinylene oligomer, 5PV as the electron donor (4×10^{-5} M) along with 8×10^{-3} M NI acceptor. The second control composite contains 10^{-5} M BEH-PPV polymer with no NI present.

The free energy change for the photoinduced electron transfer reaction: ^{1*}(BEH-PPV) + NI → (BEH-PPV)$^+$ + NI$^-$ is −1.0 eV. The free energy change for the photoinduced electron transfer reaction: ^{1*}5PV + NI → 5PV$^+$ + NI$^-$ is −1.3 eV, and is comparable to that for the BEH-PPV/NI pair. The oxidation potentials, E_{OX} of BEH-PPV and 5PV are both 0.9 V vs SCE, respectively, as determined by cyclic voltammetry. Their lowest excited state energies, E_S are 2.4 eV and 2.7 eV, respectively, as determined by the average of the energies of the lowest energy absorption and singlet excited state emission. The reduction potential, E_{RED} of NI is −0.5 V vs SCE, and ΔG for photoinduced electron transfer is estimated as $E_{OX} - E_{RED} - E_S$.

Within these composites, the energy level diagram detailing the generation of ions in the material is illustrated in Figure 4. Photoexcitation of the donor molecule (D), such as BEH-PPV, is followed by collisional interactions with the neutral electron acceptor (A) molecules, NI. This is followed by charge transfer and the generation of an ion pair. The free energies for charge separation and charge return are designed so that the free energy of charge separation is relatively low

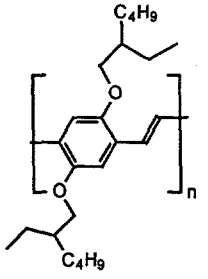

BEH-PPV

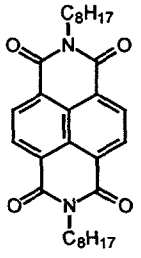

NI

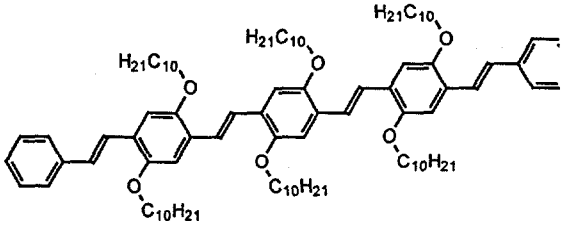

5PV

Figure 2. The BEH-PPV and 5PV molecules that function as the sensitizing chromophores and electron donors are illustrated.

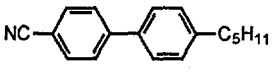

5CB

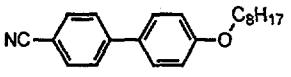

8OCB

Figure 3. The NI electron acceptor and the two components of the liquid crystal composite are shown.

compared to the free energy for charge return. The large free energy for charge return ensures that this reaction rate (k_{CR}) will be slow, consistent with the "inverted regime" in Marcus electron transfer theory. This long lived ion pair permits enough time for solvent separated ions to form (k_{SEP}), which can then contribute to the modulated spatial charge separation that induces the photorefractive effect. On the other hand, the free energy for charge separation is large enough to provide efficient charge separation and a fast rate of charge separation, k_{CS}.

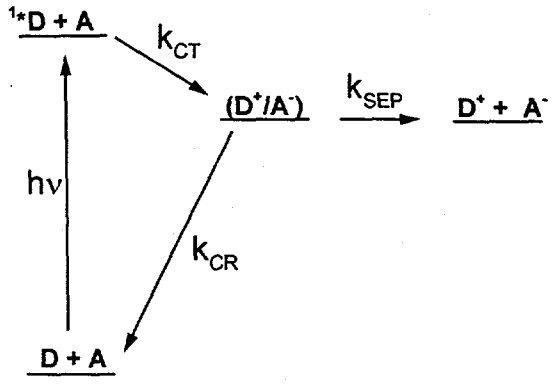

Figure 4. The energy level scheme for the photogeneration of solvent separated ions is shown.

The liquid crystal composites are sandwiched between two indium tin oxide coated glass slides that are functionalized with n-octadecylsilyl groups to induce homeotropic alignment.[16] The cell thickness is 26 μm as determined by a Teflon spacer. The concentrations of BEH-PPV and 5PV used in these experiments provide equal absorbances of A = 0.02 at 514 nm. A 1.5 V potential is applied to the cell to induce both directional charge transport and the orientational photorefractive effect.[13] All of the composites exhibit a dark conductivity of approximately $4x10^{-11}$ S·cm^{-1}. The photoconductivities of the composites using 514 nm, 1W·cm^{-2} irradiation are $1x10^{-10}$ S·cm^{-1} for both BEH-PPV/NI and 5PV/NI, and 3×10^{-11} S·cm^{-1} for the composite containing BEH-PPV alone.

The experimental configuration for the photorefractive experiment is shown in Figure 5. Two coherent laser beams from an Ar^+ laser with 1 mW total power at 514 nm and a beam diameter of 2.5 mm are overlapped in the sample to create an optical interference pattern.[9] For these composites, asymmetric energy transfer (beam coupling) from one of the crossed laser beams to the other is observed. This phenomenon is characteristic for the photorefractive effect, wherein the refractive index grating is phase shifted relative to the interference pattern.[30] Our experiments span the range of volume (Bragg) gratings at small Λ to thin (Raman-Nath) gratings at large Λ. In the thin grating regime, other phenomena can also lead to the observation of asymmetric beam coupling, including thermal, photochromic, order-disorder, and phase change effects.[24] However, these possibilities are ruled out using diagnostic experiments that have been discussed previously.[16, 21, 31] First, photorefractivity is not observed unless a static electric field is present, suggesting that a static internal field, such as a space charge field, is present that leads to director axis reorientation. No effect is observed for an ac applied electric field. Second, the sample must be tilted relative the writing beams' bisector, as shown in Fig. 5, in order to see the effects. This indicates that a component of the grating wavevector must lie along the direction of the applied electric field in order for directional charge transport to occur along the wavevector. Third, a grating is only observed when the grating wavevector and the polarization lie in the same direction, indicating that the index change is a result of reorientation of the liquid crystal molecules in the plane of the two writing beams[8, 31]. None of the previously observed alternative effects can be explained by these observations. As noted in other photorefractive studies in thin media, such as semiconductor quantum wells, the direction of beam coupling in both thin and thick grating regimes has the same dependence on the polarity of the space-charge field.[32]

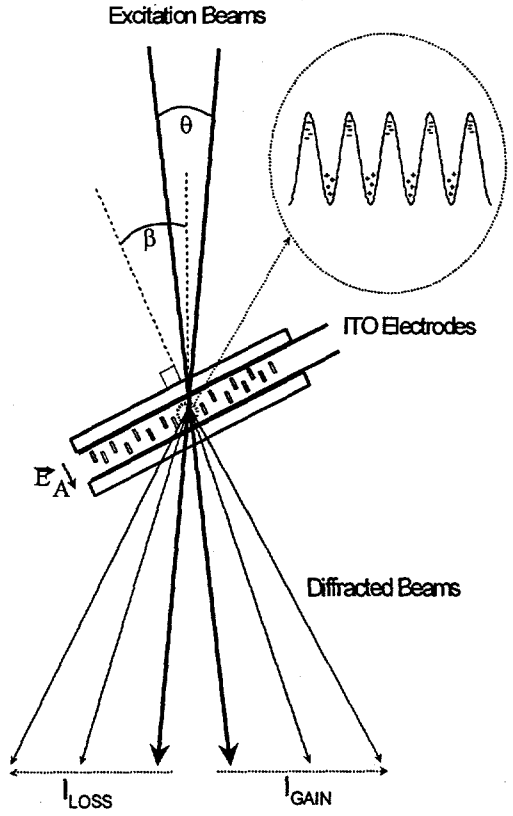

Figure 5. The experimental configuration for the two beam coupling experiment is shown.

3. RESULTS AND DISCUSSION

Figures 6 and 7 show the kinetics of beam coupling for two different values of Λ in the BEH-PPV/NI composite and the control composite containing 5PV/NI. The beam coupling ratio for beam 1 is I_{12}/I_1, where I_{12} is the intensity of beam 1, when both beam 1 and beam 2 are present in the sample, and I_1 is the intensity of beam 1 in the absence of beam 2. The corresponding beam coupling ratio for beam 2 is I_{21}/I_2, where I_{21} is the intensity of beam 2, when both beam 1 and beam 2 are present in the sample, and I_2 is the intensity of beam 2 in the absence of beam 1. Open symbols indicate the same beam, while solid symbols indicate the other beam. For each curve a photodiode monitors the intensity of one beam, while the other beam is incident on the sample at 5 s and blocked at 20 s. Comparing the data illustrated in Figure 6 with that in Figure 7, the direction of beam coupling at smaller Λ is the same for both composites, while it is opposite for the two composites at larger Λ. Comparing Figures 8a and 8b for Λ < 5.5 μm, the direction of beam coupling in the BEH-PPV/NI composite is the same as that of the 5PV/NI control composite. A further observation is that beam coupling is observed in the BEH-PPV/NI composite at the high resolution Λ = 1.5 μm, whereas the smallest Λ achieved with the 5PV/NI composite is 3 μm. These observations are consistent with a space-charge field created through an ion diffusion mechanism. Within this model, the magnitude of the space charge field in liquid crystals increases as the difference between the diffusion coefficients for the cation and anion increases.[21, 31] NI^- has a larger diffusion coefficient than oxidized electron donors of comparable size, including $5PV^+$.[10, 11] Since BEH-PPV$^+$ polymer cation has a much smaller diffusion coefficent than $5PV^+$, the space-charge fields derived from diffusion within both the BEH-PPV/NI and 5PV/NI composites should have the same polarity, and therefore, the same asymmetric energy exchange direction. The larger size and smaller diffusion coefficient of BEH-PPV$^+$ relative to that of $5PV^+$ results in a higher resolution grating attained with the BEH-PPV/NI composite because the difference in diffusion coefficients between BEH-PPV$^+$ and NI^- is larger than that between $5PV^+$ and NI^-.

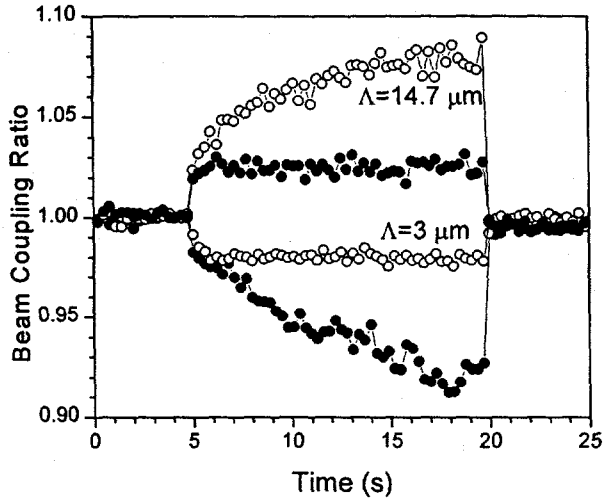

Figure 6. The kinetics of beam coupling in the BEH-PPV/NI liquid crystal composite is shown for Λ=14.7 μm (□ and ■) and 3.0 μm (○ and ●).

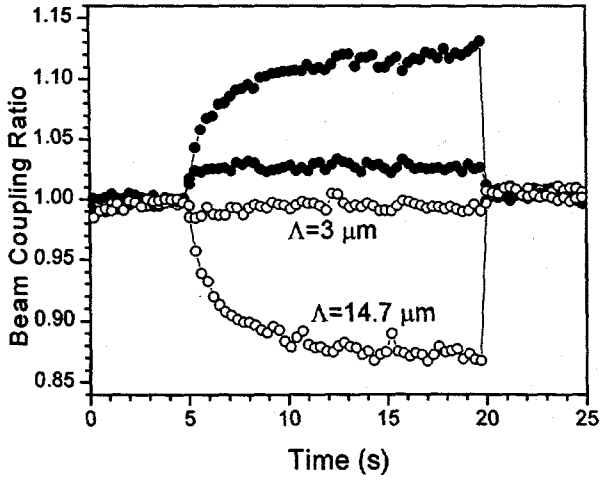

Figure 7. The kinetics of beam coupling in the 5PV/NI liquid crystal composite is shown for Λ=14.7 μm (□ and ■) and 3.0 μm (○ and ●).

The BEH-PPV/NI composite at Λ = 1.5 μm functions in the Bragg, thick grating regime. Operating a photorefractive device in the Bragg regime is essential to carry out holographic information storage in these materials. The quality factor, Q that determines whether the grating is in the Bragg diffraction regime is given as $Q=2\pi D\lambda/\Lambda^2 n$, where D is the optical path length (for a tilt angle 30° relative to homeotropic direction of the cell, D=26μm/cos30°=30μm), λ is the wavelength, and n is the refractive index. Q>>1 is indicative of a Bragg

regime grating. At Λ=1.5 μm, Q=25 and is comparable to typical Q values for photorefractive gratings in polymers, where $\Lambda \approx 3$ μm and $D \approx 100$ μm.

The sign of the asymmetric beam coupling inverts for the BEH-PPV/NI composite at approximately Λ = 5.5 μm, while neither control composite shows this inversion. This suggests that the polarity of the space-charge field inverts at this point.[30] Comparing Figures 8a and 8b for $\Lambda > 5.5$ μm, the direction of beam coupling in the BEH-PPV/NI composite is the same as that with the control composite containing BEH-PPV alone. This indicates that the sign of the mobile charge carrier that contributes to space-charge field formation is the same for $\Lambda > 5.5$ μm in these two composites, and opposite to that for the control composite containing 5PV/NI. Therefore, since negative charges carried by diffusing NI^- are the most mobile charges that contribute to a phase-shifted space-charge field in the BEH-PPV/NI composite for $\Lambda < 5.5$ μm, positive charges are the most mobile charges that contribute to a phase-shifted space-charge field at $\Lambda > 5.5$ μm.

Since the high 200 kD molecular weight of $BEH\text{-}PPV^+$ precludes rapid ion diffusion, a charge migration mechanism other than diffusion is producing the space-charge field at larger values of Λ. Solutions of alkoxylated PPVs display very high intra-chain mobilities for both holes and electrons.[27, 33] Fast hole transport along the BEH-PPV chain, coupled with hole hopping to other BEH-PPV chains can lead to long distance hole migration in the composite. This mechanism of charge transport can be considered a charge drift mechanism in the trap density limited regime. This means that the charge drift length, L_E, is larger in the BEH-PPV doped liquid crystals relative to the 5PV doped liquid crystals. In the context of equation 3, it is likely that $\tau^{\pm}$ and $\mu^{\pm}$ are significantly enhanced in the BEH-PPV polymer due to the delocalization of charge and fast intrachain hole mobilities. The increase in $\tau^{\pm}$ and $\mu^{\pm}$ through this mechanism is not possible for smaller cations and anions such as $5PV^+$ and NI^-. Furthermore, the magnitude of the current density due to drift should be larger (eq. 2) in BEH-PPV doped composites because $n^{\pm}$ is proportional to the carrier lifetime.[25] Thus, L_E and $n^{\pm}$ are large enough in the BEH-PPV composite to observe charge drift as a contributor to space-charge field formation for the first time in liquid crystals.

The fringe spacing limit in which each charge transport mechanism dominates is consistent with our analysis. The contribution to the magnitude of the space-charge field derived from ion diffusion is inversely proportional to Λ.[21, 31] However, the contribution to the space-charge field magnitude from charge drift, in the trap density limited model, is independent of Λ to a first approximation.[25] The space-charge field due to drift can contribute to the photorefractive grating as long as $2\pi L_E \geq \Lambda$ so that the space-charge field is phase-shifted from the optical interference pattern. Therefore, in the BEH-PPV polymer/liquid crystal composites where L_E is enhanced, the charge drift mechanism should dominate space-charge field formation at the larger values of Λ explored in our experiments, but the ion diffusion mechanism should dominate at smaller Λ (Figure 8). Furthermore, the fact that the control composite containing only BEH-PPV does not show any beam coupling below 5.5 μm is consistent with the availability of only one charge transport mechanism, charge drift, because the absence of NI^- precludes diffusional space charge fields at lower values of Λ. This discussion only applies to which charge transport mechanism will dominate space-charge field formation at a given fringe spacing. The magnitude of the space-charge field does not correlate with the beam coupling magnitude, because the orientational

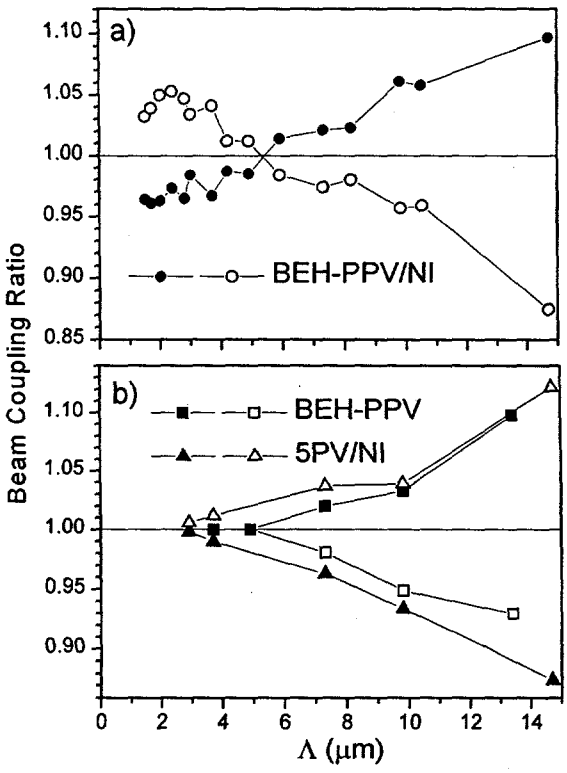

Figure 8. a)The magnitude and direction of beam coupling in the BEH-PPV/NI liquid crystal composite is shown. b) The beam coupling ratio vs Λ for the control composites containing only BEH-PPV or 5PV/NI is shown. Open symbols indicate the same beam for all three composites, while solid symbols indicate the other beam.

response of liquid crystals decreases at smaller fringe spacings for $\Lambda<2d$.[31]

4. CONCLUSIONS

We have shown that the BEH-PPV conjugated polymer provides a mechanism to enhance the photorefractive effect in each fringe spacing limit. In the ion diffusion limit, the much lower mobility of BEH-PPV$^+$ relative to that of NI$^-$ decreases the fringe spacing in which photorefractive beam coupling can be observed. Furthermore, the use of BEH-PPV enhances the charge drift length so that a new space-charge field generation mechanism in liquid crystals becomes possible. The versatility of conjugated polymers in enhancing the photorefractive effect in liquid crystal composites may lead to the development of new optical devices that use photorefractivity for information processing and storage.

ACKNOWLEDGMENTS

We gratefully acknowledge support from the Technology Research Division, Office of Advanced Scientific Computing Research, U.S. Department of Energy, under contract W-31-109-ENG-38 (GPW) and the Office of Naval Research under grant No. N00014-99-1-0411 (MRW).

REFERENCES

1. L. Solymar, D. J. Webb, and A. Grunnet-Jepsen, "The physics and applications of photorefractive materials". Oxford: Clarendon Press, 1996.
2. W. E. Moerner and S. M. Silence, "Polymeric Photorefractive Materials," *Chem. Rev.* **94**, pp. 127-155, 1994.
3. Y. Zhang, Y. Cui, and P. N. Prasad, "Observation of Photorefractivity in a Fullerene-Doped Polymer Composite," *Phys. Rev. B* **46**, pp. 9900, 1992.
4. B. L. Volodin, B. Kippelen, K. Meerholz, B. Javidi, and N. Peyghambarian, "A Polymeric Optical Pattern Recognition System for Security Verification," *Nature* **383**, pp. 58-60, 1996.
5. S. Ducharme, J. C. Scott, R. J. Twieg, and W. E. Moerner, "Observation of the Photorefractive Effect in a Polymer," *Phys. Rev. Lett.* **66**, pp. 1846-1849, 1991.
6. L. Yu, W. K. Chan, A. Peng, and A. Gharavi, "Multifunctional Polymers Exhibiting Photorefractive Effects," *Acc. Chem. Res.* **29**, pp. 13-21, 1996.
7. I. C. Khoo, H. Li, and Y. Liang, "Observation of Orientational Photorefractive Effects in Nematic Liquid Crystals," *Opt. Lett.* **19**, pp. 1723-25, 1994.
8. E. V. Rudenko and A. V. Sukhov, "Photoinduced Electrical Conductivity and Photorefraction in a Nematic Liquid Crystal," *JETP Lett.* **59**, pp. 142-46, 1994.
9. G. P. Wiederrecht, B. A. Yoon, and M. R. Wasielewski, "High Photorefractive Gain in Nematic Liquid Crystals Doped with Electron Donor and Electron Acceptor Molecules," *Science* **270**, pp. 1794-97, 1995.
10. G. P. Wiederrecht, B. A. Yoon, and M. R. Wasielewski, "Photorefractive Liquid Crystals," *Adv. Mat.* **8**, pp. 535-39, 1996.
11. G. P. Wiederrecht, B. A. Yoon, and M. R. Wasielewski, "Photorefractive Liquid Crystals Doped with Electron Donor and Acceptor Molecules," *Synth. Met.* **84**, pp. 901-2, 1997.
12. G. P. Wiederrecht, B. A. Yoon, W. A. Svec, and M. R. Wasielewski, "Photorefractivity in nematic liquid crystals containing electron donor-acceptor molecules that undergo intramolecular charge separation," *J. Am. Chem. Soc.* **119**, pp. 3358-3364, 1997.
13. W. E. Moerner, S. M. Silence, F. Hache, and G. C. Bjorklund, "Orientationally Enhanced Photorefractive Effect in Polymers," *J. Opt. Soc. Am. B* **11**, pp. 320-30, 1994.
14. K. Meerholz, B. L. Volodin, Sandalphon, B. Kippelen, and N. Peyghambarian, "A Photorefractive Polymer with High Optical Gain and Diffraction Efficiency near 100%," *Nature* **371**, pp. 497-500, 1994.
15. A. Grunnet-Jepsen, C. L. Thompson, R. J. Twieg, and W. E. Moerner, "High performance photorefractive polymer with improved stability," *Appl. Phys. Lett.* **70**, pp. 1515-1517, 1997.
16. G. P. Wiederrecht and M. R. Wasielewski, "Photorefractivity in Polymer-Stabilized Nematic Liquid Crystals," *J. Am. Chem. Soc.* **120**, pp. 3231-3236, 1998.
17. A. Golemme, B. L. Volodin, B. Kippelen, and N. Peyghambarian, "Photorefractive polymer-dispersed liquid crystals," *Opt. Lett.* **22**, pp. 1226-28, 1997.

18. H. Ono, I. Saito, and N. Kawatsuki, "Photorefractive Bragg diffraction in high- and low-molar-mass liquid crystal mixtures," *Appl. Phys. Lett.* **72**, pp. 1942-44, 1998.
19. P. M. Lundquist, R. Wortmann, C. Geletneky, R. J. Twieg, M. Jurich, V. Y. Lee, C. R. Moylan, and D. M. Burland, "Organic Glasses: A New Class of Photorefractive Materials," *Science* **274**, pp. 1182-85, 1996.
20. I. C. Khoo, S. Slussarenko, B. D. Guenther, M.-Y. Shih, P. Chen, and W. V. Wood, "Optically induced space-charge fields, dc voltage, and extraordinarily large nonlinearity in dye-doped nematic liquid crystals," *Opt. Lett.* **23**, pp. 253-255, 1998.
21. E. V. Rudenko and A. V. Sukhov, "Optically induced spatial charge separation in a nematic and resultant orientational nonlinearity," *JETP* **78**, pp. 875-882, 1994.
22. Q. Wang, L. M. Wang, and L. P. Yu, "Synthesis and Unusual Physical Behavior of a Photorefractive Polymer Containing Tris(bipyridyl)ruthenium(II) Complexes as a Photosensitizer and Exhibiting a Low Glass-Transition Temperature.," *J. Am. Chem. Soc* **120**, pp. 12860-12868, 1998.
23. N. V. Tabiryan and C. Umeton, "Surface-activated photorefractivity and electro-optic phenomena in liquid crystals," *J. Opt. Soc. Am. B* **15**, pp. 1912-17, 1998.
24. I. C. Khoo, "Holographic Grating Formation in Dye- and Fullerene C60-doped Nematic Liquid-Crystal Film," *Opt. Lett.* **20**, pp. 2137-39, 1995.
25. P. Gunter, "Holography, coherent light amplification and optical phase conjugation with photorefractive materials," *Phys. Rep.* **93**, pp. 199-299, 1982.
26. B. Maximus, E. D. Ley, A. D. Meyere, and H. Pauwels, "Ion transport in SSFLCD's," *Ferroelectrics* **121**, pp. 103-112, 1991.
27. R. J. O. M. Hoofman, M. P. d. Haas, L. D. A. Siebbeles, and J. M. Warman, "Highly mobile electrons and holes on isolated chains of the semiconducting polymer poly(phenylene vinylene)," *Nature* **392**, pp. 54-56, 1998.
28. B. Wang and M. R. Wasielewski, "Design and synthesis of metal ion-recognition-induced conjugated polymers: an approach to metal ion sensory materials," *J. Am. Chem. Soc.* **119**, pp. 12-21, 1997.
29. S. R. Greenfield, W. A. Svec, D. Gosztola, and M. R. Wasielewski, "MultiStep Photochemical Charge Separation in Rod-Like Molecules Based on Aromatic Imides and Diimides.," *J. Am. Chem. Soc.* **118**, pp. 6767-6777, 1996.
30. P. Gunter and J. P. Huignard, "Photorefractive Materials and Their Applications 1: Fundamental Phenomena". Berlin: Springer-Verlag, 1988.
31. I. C. Khoo, "Orientational Photorefractive Effects in Nematic Liquid Crystal Films," *IEEE J. Quant. Elec.* **32**, pp. 525-534, 1996.
32. Q. Wang, R. M. Brubaker, D. D. Nolte, and M. R. Melloch, "Photorefractive quantum wells: transverse Franz-Keldysh geometry," *J. Opt. Soc. Am. B* **9**, pp. 1626-41, 1992.
33. W. B. Davis, W. A. Svec, M. A. Ratner, and M. R. Wasielewski, "Distance dependence of photoinduced electron transfer through phenylenevinylene molecular wires," *Nature* **396**, pp. 60-63, 1998.